

Fiber Motion and Rheology of Suspensions with Uniform Fiber Orientation

SILVIA E. BARBOSA, MIGUEL A. BIBBÓ*

PLAPIQUI (UNS-CONICET), C.C. 717, Bahía Blanca 8000, Argentina

Received 2 September 1999; revised 5 April 2000; accepted 18 April 2000

ABSTRACT: One of the main goals in the studies of fiber suspensions is the prediction of fiber orientation in a short fiber composite part, using the processing variables, mold geometry, and material characteristics. The rheological properties of the fiber suspensions are strongly associated with the fiber orientation distribution. The understanding of the relations between the fiber structure in the suspension and its rheological properties is a key step in the design and implementation of processing operations. The fiber motion in shear flow is analyzed in this article. The study is focused on the relation between fiber orientation and rheological properties for a suspension with uniform (delta function) fiber orientation distribution in a Newtonian fluid. The study shows that the rheological properties of the suspension, measured during the start up of steady shear flow, can be used to determine the fiber orientation in the sample. The first normal stress coefficient is the property to measure in order to determine whether or not the suspension has a random fiber orientation. Any of the shear flow transient rheological properties can be used to determine the fiber initial orientation. It was found that the normal stress coefficients can show negative or positive values depending on the fiber orientation. © 2000 John Wiley & Sons, Inc. *J Polym Sci B: Polym Phys* 38: 1788–1799, 2000

Keywords: short fiber composites; fiber motion; fiber orientation; fiber suspensions; rheology of fiber suspensions

INTRODUCTION

There is currently great interest in the flow of concentrated suspensions of fibers in Newtonian solvents and polymers, because these composites can provide lightweight, strong substitutes for metals in many manufacturing operations.

Whereas processability is the main advantage of short fiber composites, the mechanical properties of the final product are strongly related to the fiber orientation distribution, which is determined during the processing. The extent to which these composites can be used is pres-

ently limited to a large degree by our understanding of the rheology of the composites and our ability to exploit the rheological properties in the design and implementation of processing operations. Ability to predict and control the distribution of fiber orientations in the final part depends on the rheological description of these suspensions plus the ability to simulate flows of suspensions numerically. Currently, satisfactory fiber configuration designs are arrived at by trial and error procedures, which can be quite costly.

The understanding of the relation between the fiber structure in the suspension and its rheological properties is a key step in the design and implementation of processing operations. Basically, the principal approaches to describe these relations are the following.

* Present address: PASA, Maipú 1, Buenos Aires, Argentina
Correspondence to: S. E. Barbosa (E-mail: sbarbosa@plapiqui.edu.ar)

Journal of Polymer Science: Part B: Polymer Physics, Vol. 38, 1788–1799 (2000)
© 2000 John Wiley & Sons, Inc.

The “hydrodynamic approach” where the forerunner was Jeffery.¹ In 1922, he calculated the instantaneous angular velocity of a neutrally buoyant ellipsoid in a Newtonian medium under creeping flow. In 1970, Batchelor^{2,3} developed a generalized equation for the hydrodynamic stress for a suspension of long axisymmetric rigid particles with negligible inertia, subject to a constant strain rate. Dinh and Armstrong,⁴ extending Batchelor’s approach and using Jeffery’s equation, have developed a constitutive equation for semiconcentrated suspensions of rigid fibers with infinite aspect ratio (L/D) in a Newtonian solvent undergoing homogeneous flows. It has been shown^{5–10} that the model prediction is in excellent agreement with the complex rheological behavior, which is a strong indication that the constitutive equation is capturing the important physics of the problem. Ausias et al.¹¹ using a similar approach to Dinh and Armstrong, developed a model for dilute suspensions of long rigid fibers and extended it to concentrated suspensions. They introduced one parameter to relate the coupling between stress and fiber orientation.

Folgar and Tucker¹² proposed a phenomenological approach to model fiber rotations based on the combination of two effects: a diffusion effect, which takes into account fiber–fiber interactions and a convection effect, which depends on the flow field applied. They introduced an empirical coefficient to take into account the effects of the suspension parameters in the interaction. Other authors^{13–15} followed a similar approach extending the model to higher fiber concentrations.

Bercraft and Metzner¹⁶ performed a “molecular approach” based on a modification of the molecular theory of Doi for liquid crystalline polymers^{17,18} to take into account the macroscopic dimensions of the fibers. They obtained good predictions for steady rheological measurements.

The last model, reported by Ghosh et al.,¹⁹ is a “thermodynamics approach”. They developed the model using a conformational tensor to represent a fiber orientation in orientation space and a Hamiltonian structure to derive the evolution of the conformation tensor. They avoided numerical problems, and with fitting parameters they have been able to predict rheological properties in steady state.

We compare the fiber motion predicted by the Dinh and Armstrong equation with that of Jeffery’s model, which has been developed for dilute suspensions with finite fiber aspect ratio. We analyze the fiber contribution to the rheology of the

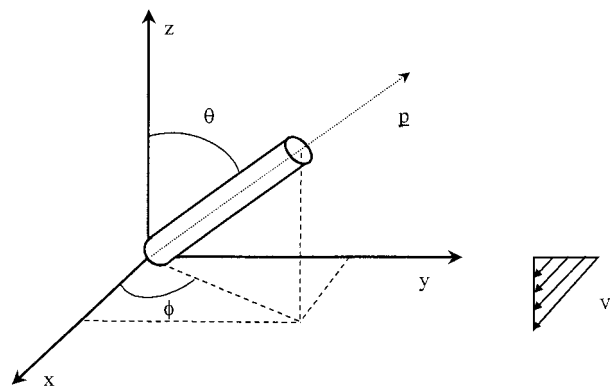


Figure 1. Fiber in shear flow: $v_x = \dot{\gamma}y$, $v_y = v_z = 0$. θ and ϕ are the spherical polar angles that describe the orientation of the fiber.

suspensions. Comparison is made between uniform and random initial fiber orientation distribution.

We prepare a method to determine whether a suspension has a random fiber orientation distribution or not, and how the angles that describe the orientation can be obtained if the suspension has a predominant alignment.

FIBER MOTION IN START-UP OF STEADY SHEAR FLOW

We consider here a homogeneous shear flow, $v_x = \dot{\gamma}y$, $v_y = v_z = 0$ where the shear rate $\dot{\gamma} = 0$ for $t \leq 0$ and is a constant for $t > 0$. The fiber structure is described by a distribution function, $\psi(\theta, \phi)$, which is a probability density, and $\psi(\theta, \phi)d\theta d\phi$ representing the probability of finding a fiber with orientation angles in a range $d\theta$ and $d\phi$ around θ and ϕ . In Figure 1 we show the angles θ and ϕ , which describe the fiber orientation and the velocity profile $v_x = \dot{\gamma}y$ in a fixed coordinate system. For this flow field the distribution function is given by:

$$\psi(\theta, \phi) = [4\pi(1 - \gamma \sin^2\theta \sin 2\phi + \gamma^2 \sin^2\theta \sin^2\phi)^{3/2}]^{-1} \quad (1)$$

where $\gamma = \dot{\gamma}t$ is the shear strain accumulated from the inception of the flow at $t = 0$. In obtaining eq 1, it is assumed that $\psi(t = 0) = 1/4\pi$, that is, that the fibers are initially randomly oriented.⁴

The equations of motion for the fiber, in terms of the spherical angles, are

$$\frac{d\theta}{d\gamma} = \sin \theta \cos \theta \cos \phi \quad (2)$$

$$\frac{d\phi}{d\gamma} = -\sin^2 \phi. \quad (3)$$

These equations can be integrated to give

$$\tan \theta = \tan \theta_0 [\gamma^2 \sin^2 \phi_0 + 2\gamma \sin \phi_0 \cos \phi_0 + 1]^{1/2} \quad (4)$$

$$\tan \phi = \frac{1}{\cot \phi_0 + \gamma}. \quad (5)$$

The Dinh and Armstrong model neglects the thickness of the fibers. For this reason the equations of motion, 2 and 3, are independent of the fiber aspect ratio.

The fiber motion for a very dilute suspension in a Newtonian fluid (using Jeffery's equation of motion), for the velocity field described is given by:^{20,21}

$$\frac{d\theta}{d\gamma} = \frac{[(L/D)^2 - 1]}{[(L/D)^2 + 1]} \quad (6)$$

$$\frac{d\phi}{d\gamma} = \frac{-1}{(L/D)^2 + 1} [(L/D)^2 \sin^2 \phi + \cos^2 \phi]. \quad (7)$$

Integration of these equations yields

$$\tan \theta = \frac{CL/D}{[(L/D)^2 \sin^2 \phi + \cos^2 \phi]^{1/2}} \quad (8)$$

$$\tan \phi = \frac{1}{L/D \tan \left[\gamma \frac{1}{L/D + D/L} + k \right]} \quad (9)$$

where

$$\tan k = \frac{1}{L/D \tan \phi_0} \quad (10)$$

$$C = \frac{\tan \phi_0}{[(L/D)^2 \sin^2 k + \cos^2 k]^{1/2}}. \quad (11)$$

C is known as the orbit constant, and k is the initial phase angle.

These equations, which have been obtained for particles with finite thickness show that the fiber

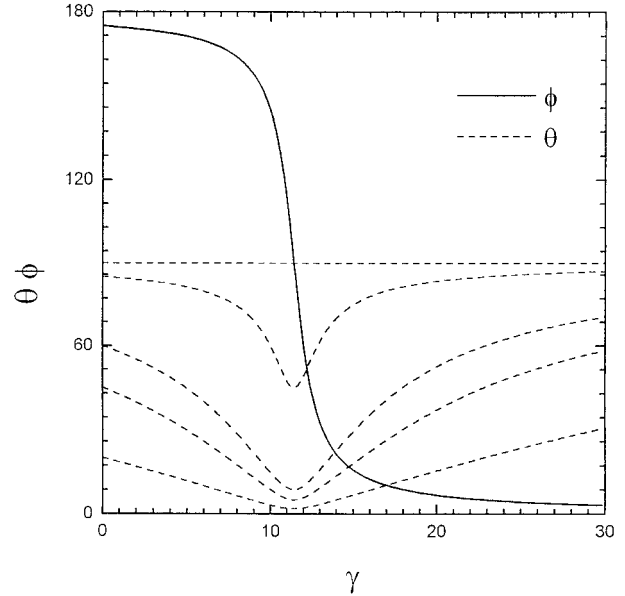


Figure 2. The change in fiber orientation, represented by the two angles θ and ϕ , during the start-up of steady shear flow for different initial fiber orientations, θ_0 and ϕ_0 , as a function of shearing strain, eqs 4 and 5. The initial orientation used was $\phi_0 = 175^\circ$ with different θ_0 : $\theta_0 = 20, 45, 60, 85,$ and 90° . The solid line is for ϕ , and dashed lines are for θ .

motion depends on the fiber aspect ratio. It is interesting to note that if the limit for $L/D \rightarrow \infty$ is taken in eqs 6 to 7, then eqs 2 and 3 are obtained.

The orientation distribution $\psi(\theta, \phi)$ completely describes the changes in the fiber structure of an initially random fiber suspension during the start-up of steady shear flow. Once the strain is specified eq 1 allows us to calculate the number of fibers in each specific orientation.

The motion of a single fiber can be studied by using eqs 4 and 5, which describe the fiber orientation as a function of the initial fiber orientation at $t = 0$ and the shear strain. The change in fiber orientation, represented by the two angles θ and ϕ , during the start-up of steady shear flow for different initial fiber orientations, θ_0 and ϕ_0 , is presented in Figure 2.

The results shown in Figure 2 are for $\phi_0 = 175^\circ$ and θ_0 between $\theta_0 = 20^\circ$ and $\theta_0 = 90^\circ$. The solid line is for ϕ , and the dashed lines are for θ . There is only one line for ϕ because the change of this angle with strain is independent of θ_0 . At the inception of the flow at $t = 0$, the fiber is very close to the shearing plane and pointing upstream. Thus during the flow the fiber will flip over and approach the shearing plane pointing down-

stream. Both angles change very slowly with γ when the fiber is close to the shearing plane, $\phi > 170^\circ$ or $\phi < 10^\circ$, but for $20^\circ < \phi < 160^\circ$, both ϕ and θ change very rapidly with γ . For all θ_0 the fiber gets the closest to the z axis when $\phi = 90^\circ$. Figure 2 shows that the fiber is moving very slowly when ϕ is close to zero; actually ϕ will go to zero only when $\gamma \rightarrow \infty$. This is a result of the assumption that the fiber has a large aspect ratio and negligible thickness; as a consequence of this the fiber will never flip over and start a new orbit. Since the fiber will never be exactly in the shearing plane, unless already there for $t = 0$, we will define a finite angular range that we will consider to be the boundary of the shearing plane. If we assume that this range is 10° , that is, the fiber is in the shearing plane when $\phi > 175^\circ$ or $\phi < 5^\circ$, then the strain units required for a fiber flip over is $\Delta\gamma \approx 25$, if the angle range is 20° then $\Delta\gamma \approx 11$. It is interesting to note that to move the fiber from $\phi = 145^\circ$ to $\phi = 45^\circ$, $\Delta\phi = 90^\circ$, only two strain units are required.

The results presented in Figure 2 can help us in understanding the experimental findings in the flow reversibility study.^{5,7} It was found that when the strain applied to the suspension is smaller than a critical value, $\gamma \approx 9$, the flow is reversible, whereas for a maximum strain larger than this critical value the flow is irreversible. From Figure 2 we can see that for $\gamma = 10$ all the fibers with ϕ_0 from 0° to approximately 135° will be aligned in the shearing plane. If the suspension had an initial random fiber orientation distribution, then at this strain, $\gamma = 10$, 75% of the fibers would have an orientation angle $\phi \approx 0^\circ$ and would thus be moving very slowly. The other 25% of the fibers with ϕ_0 between 135° and 180° have an orientation angle $\phi \approx 90^\circ$ and are moving very rapidly towards the shearing plane. Thus there is an important difference in the fiber structure for strains less than or greater than 10, and this may be associated with the fiber–fiber interaction in the suspension. For $\gamma < 10$ the fibers are all rotating towards the shearing plane with similar velocities, and there is no fiber accumulation in any particular orientation. On the other hand for $\gamma = 10$ the fibers are rotating with very different velocities. The fibers that have accumulated in the shearing plane are almost stationary and the fibers with $\phi \approx 90^\circ$ are at their maximum rotational velocity. This would suggest that the fiber–fiber interaction at $\gamma = 10$ is much stronger than that observed for $\gamma < 10$, it is not unlikely for such strong interaction between the fibers, which may

involve even fiber–fiber contact, to be nonreversible, which would explain the existence of the critical maximum strain, $\gamma \approx 9$, found experimentally.

Figure 2 shows that the equation of motion proposed by Dinh and Armstrong predicts that after the start-up of steady shear flow, for $\gamma > 20$, the fibers are aligned in the shearing plane and stay in it forever. The equation of motion derived by Jeffery, eqs 6 to 11, which is valid for very dilute suspensions in Newtonian fluids and can be used for any fiber aspect ratio, describes how the fibers go in and out of the shearing plane.

The fiber orientation in the start-up of steady shear flow calculated using eqs 6 to 11 is presented in Figure 3. The initial fiber orientation was $\phi_0 = 175^\circ$ and $\theta_0 = 45^\circ$, and the fiber aspect ratios were $L/D = 5, 10, 20$, and 30 for Figure 3(a–d), respectively. In Figure 3(d) a calculation using the Dinh and Armstrong equation is also included. The fiber is initially close to the shearing plane pointing upstream. With increasing strain the fiber moves toward the shearing plane pointing downstream, when ϕ changes from -180° to 180° the fiber has completed an orbit. Despite the fact that the fiber motion is qualitatively the same for all four fiber aspect ratios, the number of orbits performed by the fiber when $\gamma = 100$ and the time that the fiber spends getting into and out of the shearing plane is strongly dependent on the fiber aspect ratio. The fiber is considered to be in the shearing plane when $\phi > 170^\circ$ or $\phi < 10^\circ$. For $L/D = 5$, Figure 3(a) shows that when $\gamma = 100$ the fiber has performed three orbits, and that every time that the fiber is in the shearing plane, it remains there for approximately 10 strain units. For $L/D = 10$, Figure 3(b) shows that when $\gamma = 100$ the fiber has performed 1.5 orbits, and approximately 25 strain units are required for the fiber to move in and out of the shearing plane. For $L/D = 20$, Figure 3(c) shows that when $\gamma = 100$ the fiber has performed one orbit, and approximately 50 strain units are required for the fiber to move in and out of the shearing plane. For $L/D = 30$, Figure 3(d) shows that when $\gamma = 100$ the fiber has performed 0.5 orbit, and approximately 85 strain units are required for the fiber to move in and out of the shearing plane. Figure 3(d) shows that for $L/D = 30$, the fiber motion described by the Dinh and Armstrong equations is very close to that obtained by using Jeffery's equation. Figure 3 shows clearly that for suspensions of long fibers, $L/D > 20$ with increasing γ , the particles align in the

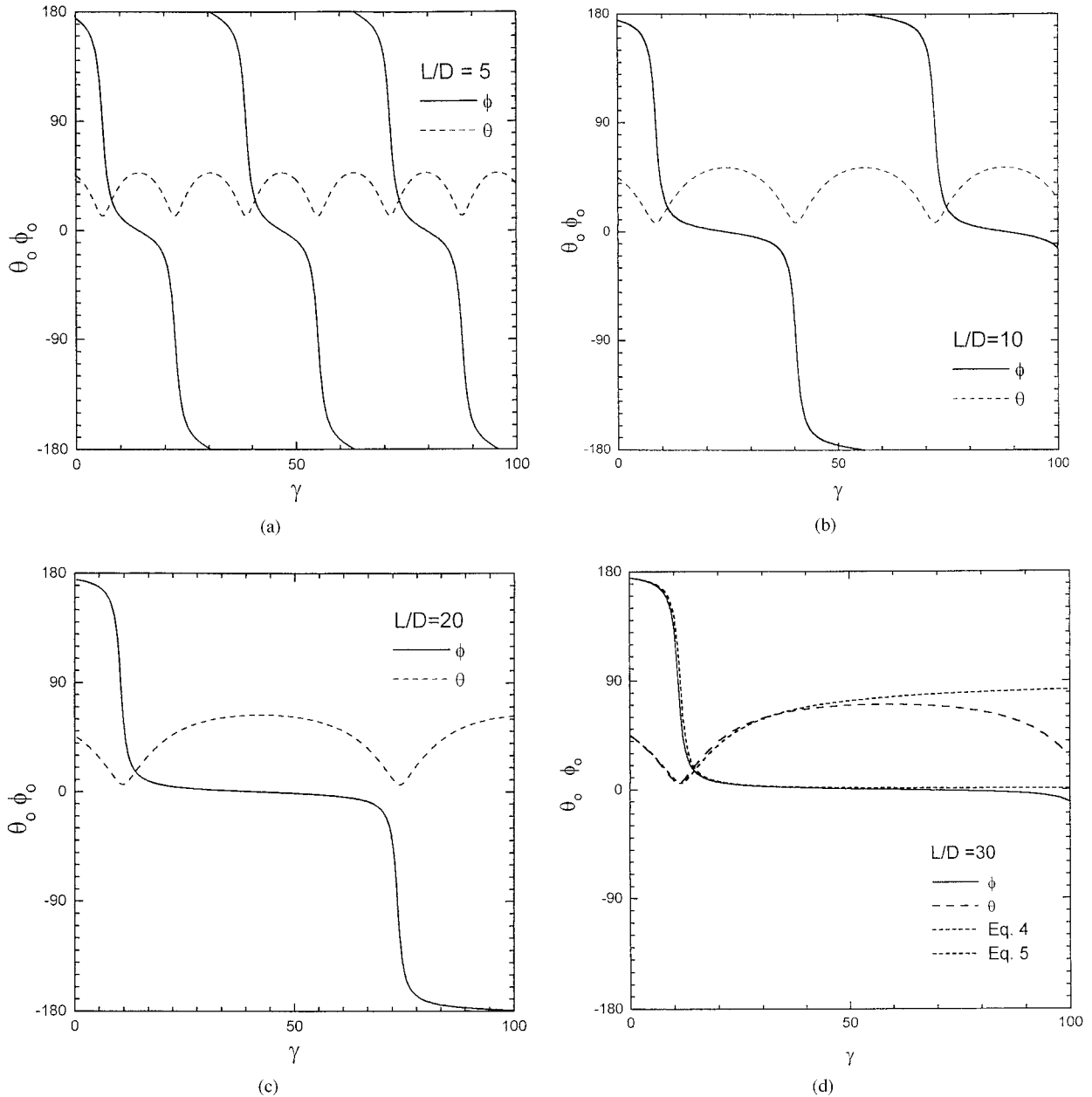


Figure 3. The change in fiber orientation, represented by the two angles θ and ϕ , during the start-up of steady shear flow for different initial fiber orientations, θ_0 and ϕ_0 , as a function of shearing strain, according to eqs 8 to 11 (Jeffery's equation). The initial orientation used was $\phi_0 = 175^\circ$ and $\theta_0 = 45^\circ$, and the fiber aspect ratio was: (a) $L/D = 5$, (b) $L/D = 10$, (c) $L/D = 20$, (d) $L/D = 30$. The solid line is for ϕ , and the dashed lines are for θ . In (d) the dotted line are eqs 4 and 5 (Dinh and Armstrong).

shearing plane; the flipping time is so small compared with the time that the fiber remains in the shearing plane that for large strain, $\gamma > 20$, the overall picture is one of a suspension with all the fibers aligned in the shearing direction. On the other hand, for suspensions of short fibers, L/D

< 20 , both times are of the same order of magnitude and for large strain all fiber orientations are present. We have noticed this different theoretical behavior when we compared the rheological properties of suspensions with different fiber aspect ratios.

RHEOLOGICAL PROPERTIES OF A SUSPENSION WITH UNIFORM FIBER ORIENTATION

The constitutive equation for a semiconcentrated fiber suspension in Newtonian fluids developed by Dinh and Armstrong, is used to describe the rheological properties of suspensions with uniform (delta function) fiber orientation distribution function.

The (extra) stress tensor τ is given by:

$$\tau = -\eta_s \dot{\gamma} - \eta_s \frac{2\pi n L^3}{12 \ln(2h/D)} \kappa : \int \mathbf{p}\mathbf{p}\mathbf{p}\mathbf{p}\psi d\mathbf{p}. \quad (12)$$

The first term on the right hand of eq 12 is the contribution to the stress from the solvent, and the second term gives the contribution from the fibers. nL^3 expresses the number of fibers present in the domain swept out by a fiber rotating around a minor axis, h is the average distance from a given fiber to its nearest neighbor,^{3,17,22,23} the unit vector \mathbf{p} gives the direction of a fiber at time t , κ is the transpose of the velocity gradient tensor and ψ is the distribution function introduced to account for the probability that the fiber selected has a specific orientation \mathbf{p} at time t . When all the fibers are oriented in the same direction, \mathbf{p}_0 , the distribution function is given by a delta function

$$\psi = \delta(\mathbf{p} - \mathbf{p}_0) \quad (13)$$

With this distribution function in eq 12 we obtain

$$\tau = -\eta_s \dot{\gamma} - \eta_s \frac{2\pi n L^3}{12 \ln(2h/D)} \kappa : \mathbf{p}_0 \mathbf{p}_0 \mathbf{p}_0 \mathbf{p}_0. \quad (14)$$

Equation 14 has been used to evaluate the rheological properties of the suspension for shear flow ($v_x = \dot{\gamma}y, v_y = v_z = 0$). The kinematics for this flow are described by:

$$\kappa = \dot{\gamma} \begin{bmatrix} 0 & 1 & 0 \\ 0 & 0 & 0 \\ 0 & 0 & 0 \end{bmatrix} \quad (15)$$

By taking the expression for κ and inserting it into eq 14, the following expressions for η^+ , Ψ_1^+ , Ψ_2^+ , and $\Psi_1^+ - \Psi_2^+$ are obtained for the fiber suspensions:

$$\left[\frac{\eta^+}{\eta_s} - 1 \right] = \frac{2\pi n L^3}{12 \ln(2h/D)} \sin^4\theta \cos^2\phi \sin^2\phi \quad (16)$$

$$\Psi_1^+ = \frac{2\pi n L^3}{12 \ln(2h/D) \dot{\gamma}} \sin^4\theta \frac{\sin 4\phi}{4} \quad (17)$$

$$\Psi_2^+ = \frac{2\pi n L^3}{12 \ln(2h/D) \dot{\gamma}} \sin^4\theta \frac{\sin 2\phi}{2} \times [\sin^2\phi - \cot^2\theta] \quad (18)$$

$$\Psi_1^+ - \Psi_2^+ = \frac{2\pi n L^3}{12 \ln(2h/D) \dot{\gamma}} \sin^4\theta \times \left[\frac{\sin 4\phi}{4} - \frac{\sin 2\phi}{2} (\sin^2\phi - \cot^2\theta) \right]. \quad (19)$$

Equations 16 to 19 describe the rheological properties of the suspension as a function of the fiber orientation. For example, eq 16 predicts the transient viscosity for a suspension with uniform fiber orientation given by the angles ϕ and θ in the inception of the shear flow. Since there is no time or strain in the equation it is only valid for that instant when all fibers have orientation θ, ϕ . These equations are useful to see how the orientation of the fiber affects the fiber contribution to the rheological properties of the suspension. If we are interested in the change of the suspension viscosity during the start-up of steady shear flow, we have to use both the equation of motion, eqs 4 and 5 and eq 16. First the initial fiber orientation is selected, ϕ_0 and θ_0 ; then by using the equation of motion we obtain ϕ and θ for each strain, and these angles are then put into eq 16 to obtain the suspension viscosity. Below we present the suspension rheological properties as functions of the orientation angles, ϕ and θ (Figs. 4 and 5) and as functions of the shearing strain in the start-up of steady shear flow for suspensions with uniform initial fiber orientation distributions (Figs. 6 to 11).

In Figure 4 the fiber contribution to the suspension viscosity is shown as a function of both orientation angles, ϕ and θ . There is no contribution to the suspension viscosity when the fibers are in the shearing plane, $\phi = 0^\circ$ or 180° for all θ , and $\theta = 0^\circ$ or 180° for all ϕ . The contribution is also zero when the fibers are perpendicular to the velocity field, $\phi = 90^\circ$ for all θ . The maximum contribution is obtained when the fibers are oriented at $\theta = 90^\circ$ and $\phi = 45^\circ$ or $\phi = 135^\circ$. Notice

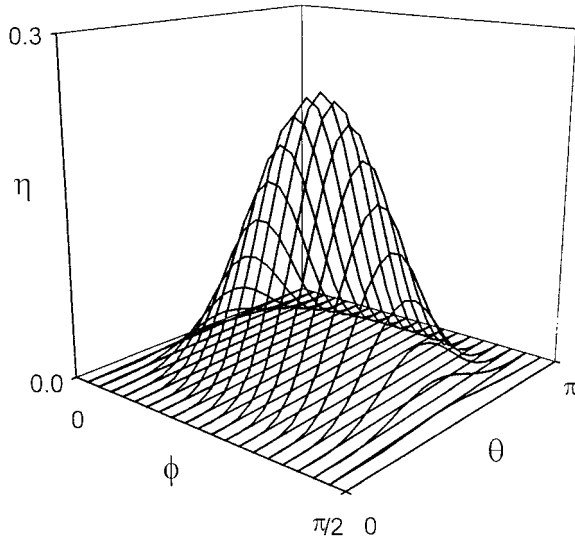


Figure 4. The dimensionless fiber contribution to the suspension viscosity as a function of θ and ϕ (eq 16).

that fibers oriented at ϕ or $\phi + \pi/2$ show the same contribution to the suspension viscosity.

In Figure 5 the first normal stress coefficient is shown as a function of both orientation angles, ϕ and θ . There are several fiber orientations for which Ψ_1^+ is zero: (a) fibers in the shearing plane, $\phi = 0^\circ$ or 180° for all θ , and $\theta = 0^\circ$ or 180° for all ϕ , (b) fibers perpendicular to the velocity field, $\phi = 90^\circ$ for all θ , and (c) fibers oriented at $\phi = 45^\circ$ or $\phi = 135^\circ$ for all θ . Fibers oriented at ϕ or $\phi + \pi/2$ show the same Ψ_1^+ . It is interesting to notice that Ψ_1^+ can be positive or negative depending on the fiber orientation. The maximum Ψ_1^+ is obtained for fibers at $\theta = 90^\circ$ and $\phi = \pi/8$ or $\phi = 5\pi/8$ and the minimums are for fibers at $\theta = 90^\circ$ and $\phi = 3\pi/8$ or $\phi = 7\pi/8$.

We have already shown how the orientation of the fiber affects the fiber contribution to the suspension rheological properties. Next we study the effect of the initial fiber orientation distribution on the suspension rheological properties in the start-up of steady shear flow. We calculate η^+ , Ψ_1^+ , Ψ_2^+ , and $\Psi_1^+ - \Psi_2^+$ using the following flow history: The suspension is first sheared in the positive direction, $v_x = \dot{\gamma}y$, up to a maximum strain $\gamma_m = 20$; the flow is then reversed, $v_x = -\dot{\gamma}y$, and the suspension is sheared up to $\gamma_m = -20$; finally the shear direction is changed again, $v_x = \dot{\gamma}y$, and the suspension is sheared until $\gamma = 0$.

Figure 6 shows the rheological properties as a function of shear strain for a suspension with initial random fiber orientation distribution. Fig-

ures 7 and 8 show the rheological properties for suspensions with an initial uniform fiber orientation distribution. At $t = 0$ all the fibers have an orientation given by $\phi_o = 90^\circ$ and $\theta_o = 90^\circ$ in Figure 7 and $\phi_o = 90^\circ$ and $\theta_o = 45^\circ$ in Figure 8. The contribution of the fibers to the suspension viscosity shows, in general, the same behavior for suspensions with both initial orientation distributions. For the initially random system the maximums are at $\gamma \approx \pm 1.3$, whereas for the initially uniform system the maximums are at $\gamma = \pm 1$. At $\gamma = 0$ the suspension viscosity is zero for the suspension with uniform orientation. This follows from the fact that we have chosen $\phi_o = 90^\circ$ for the initial orientation; any other ϕ_o will give a non-zero value, but if ϕ_o is larger than 90° η^+ will go to zero for a strain at which ϕ is 90° . The value of θ selected for the initial orientation only affects the magnitude of η^+ . The main difference between random and uniform initial distribution is perhaps the magnitude of η^+ : the maximum dimensionless contribution to the suspension viscosity is 0.085 for the random system and 0.25 for the system with uniform distribution ($\phi_o = 90^\circ$ and $\theta_o = 90^\circ$). The normal stress coefficient difference $\Psi_1^+ - \Psi_2^+$ shows a similar transient behavior for all three initial fiber orientation distributions but the magnitude of the peak depends strongly on the initial fiber distribution. The small peak that is observed in the random system at $\gamma \approx 0.5$ is one order of magnitude bigger than when the fibers are initially all aligned at ϕ_o .

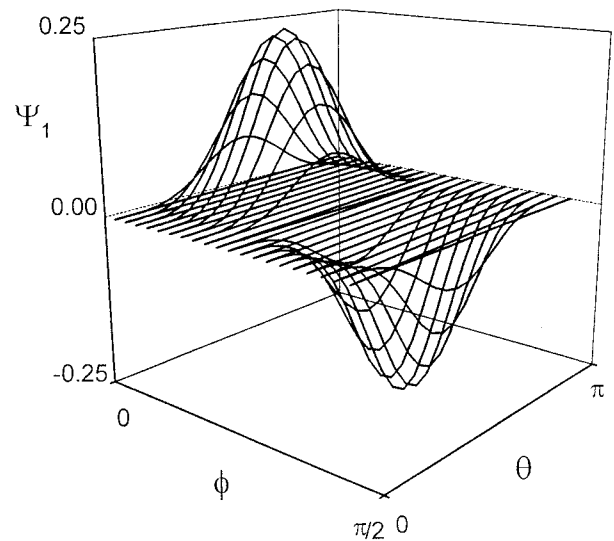


Figure 5. The dimensionless first normal stress coefficient for the suspension as a function of θ and ϕ (eq 17).

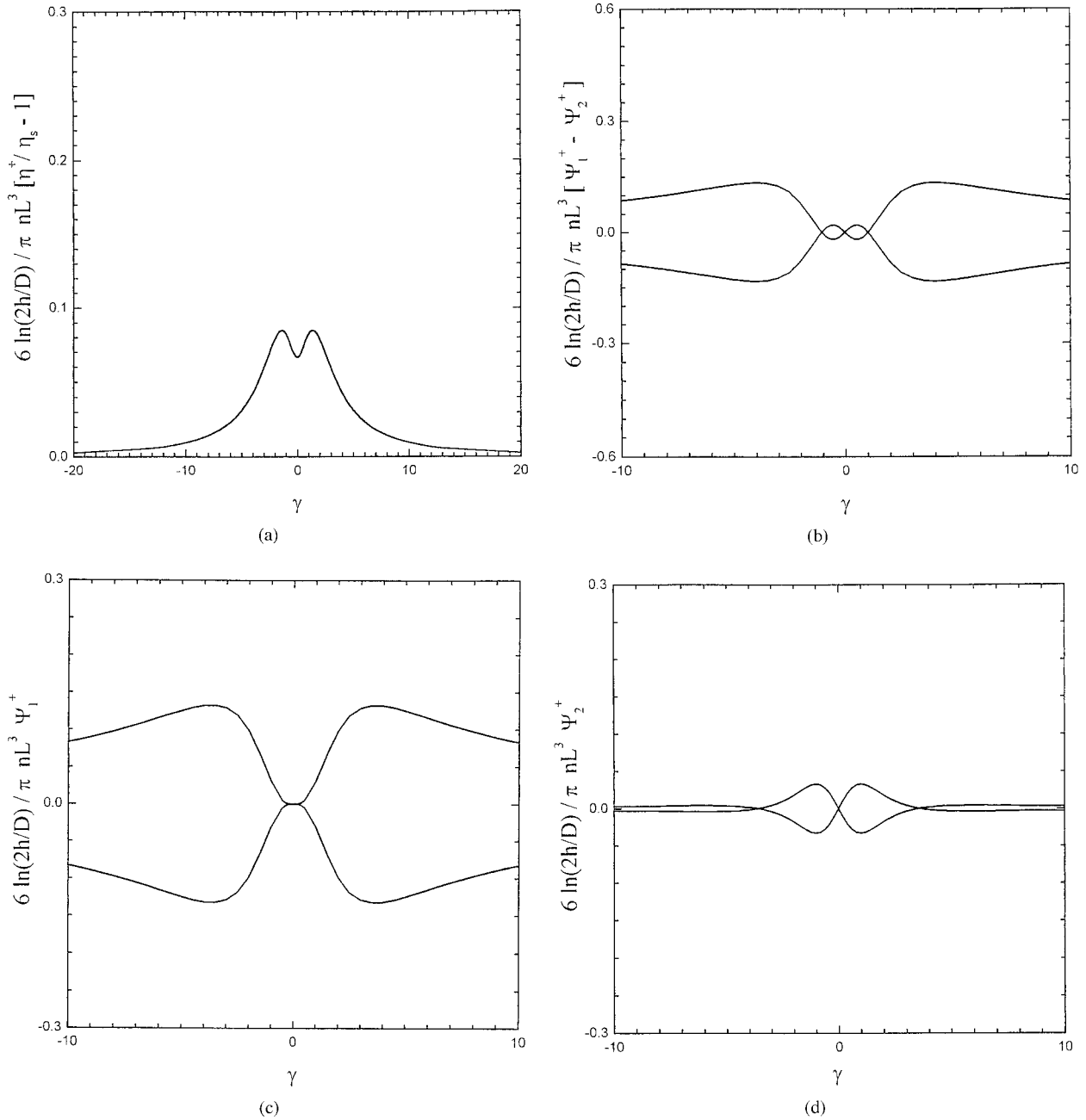


Figure 6. The dimensionless rheological properties as a function of shear strain for a suspension with initial random fiber orientation distribution in the start-up of steady shear flow. The shearing direction was changed two times. $v_x = \dot{\gamma}y$ for $\gamma = 0$ to $\gamma = 20$, $v_x = -\dot{\gamma}y$ for $\gamma = 20$ to $\gamma = -20$, and $v_x = \dot{\gamma}y$ for $\gamma = -20$ to $\gamma = 0$. (a) Fiber contribution to transient viscosity of the suspension $(\eta^+/\eta_s - 1)$; (b) normal stress coefficient difference $(\Psi_1^+ - \Psi_2^+)$; (c) first normal stress coefficient Ψ_1^+ ; and (d) second normal stress coefficient Ψ_2^+ .

$= 90^\circ$ and $\theta_o = 90^\circ$. For $\theta_o = 45^\circ$ and the peak is smaller but still larger than in the suspension with initial random orientation. The second peak in $\Psi_1^+ - \Psi_2^+$ at $\gamma \approx 3.5$ is also affected by the

initial distribution. It follows the same trend as the peak at $\gamma \approx 0.5$ but the changes in magnitude are smaller. For Ψ_1^+ the initial fiber orientation distribution has a much stronger effect. The

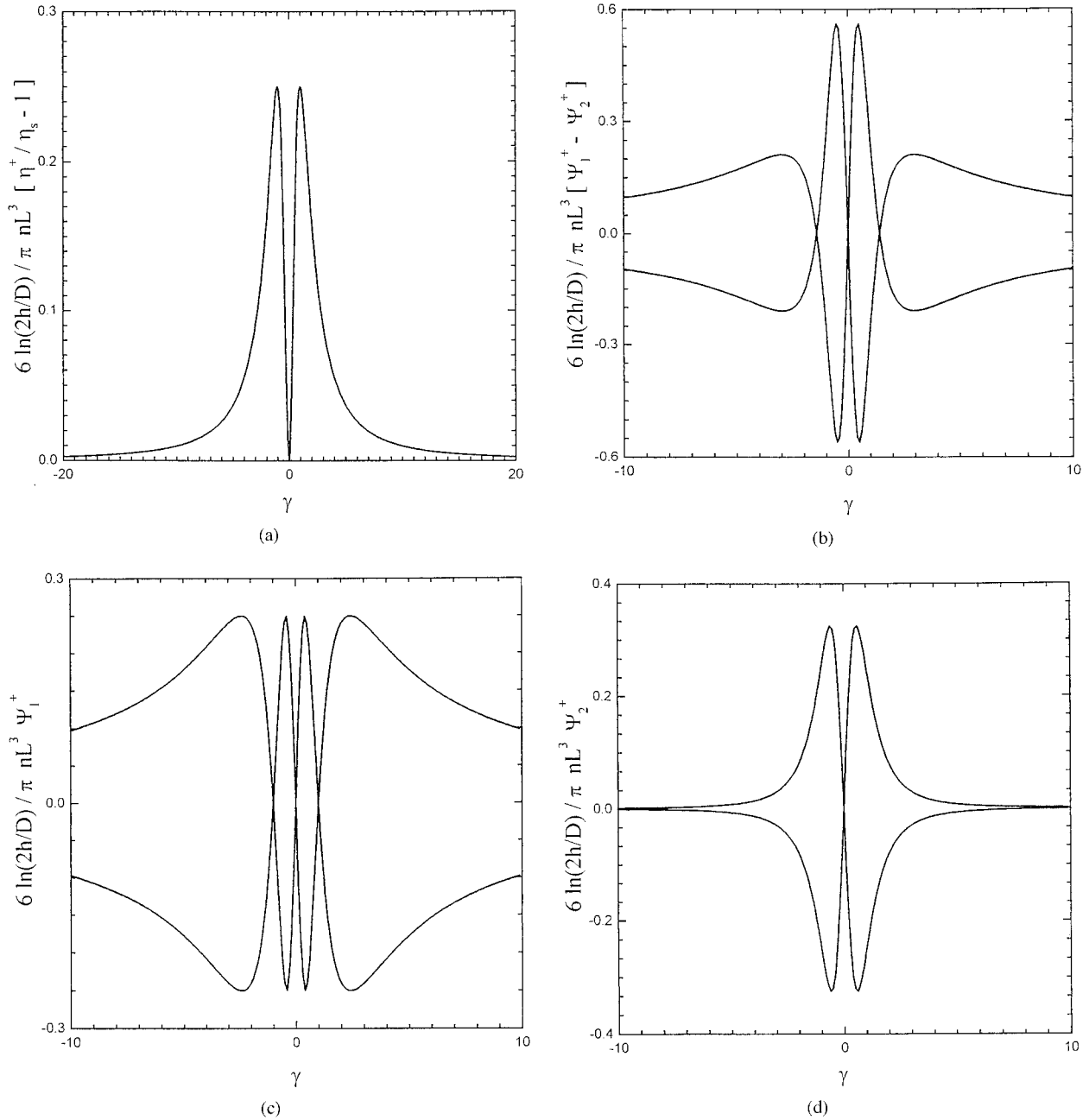


Figure 7. The dimensionless rheological properties as a function of shear strain for a suspension with uniform fiber orientation distribution, $\phi_o = 90^\circ$ and $\theta_o = 95^\circ$, in the start-up of steady shear flow. The shearing direction was changed two times. $v_x = \dot{\gamma}y$ for $\gamma = 0$ to $\gamma = 20$, $v_x = -\dot{\gamma}y$ for $\gamma = 20$ to $\gamma = -20$, and $v_x = \dot{\gamma}y$ for $\gamma = -20$ to $\gamma = 0$. (a) Fiber contribution to transient viscosity of the suspension $(\eta^+/\eta_s - 1)$; (b) Normal stress coefficient difference $(\Psi_1^+ - \Psi_2^+)$; (c) first normal stress coefficient Ψ_1^+ ; and (d) second normal stress coefficient Ψ_2^+ .

shape of the transient curve changes when the initial orientation is changed from random to uniformly aligned. The suspension with an initially random orientation distribution shows only one

peak in Ψ_1^+ , and for small strains, $\gamma = 0$ to $\gamma = 0.5$, Ψ_1^+ is very close to zero. When the fibers are initially uniformly aligned at $\phi_o = 90^\circ$ and $\theta_o = 90^\circ$, Ψ_1^+ shows two peaks; the one that is

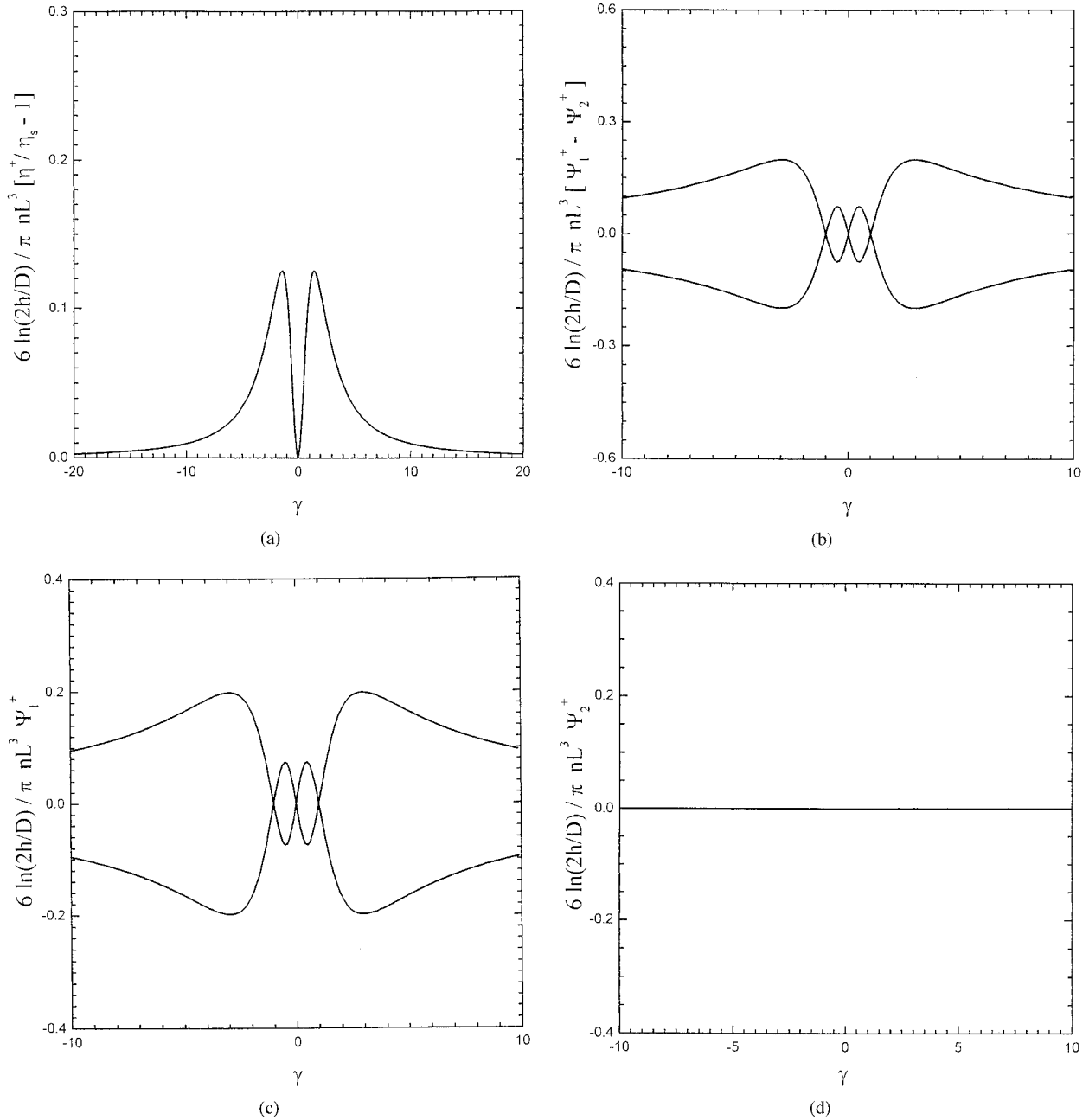


Figure 8. The dimensionless rheological properties as a function of shear strain for a suspension with uniform fiber orientation distribution, $\phi_o = 90^\circ$ and $\theta_o = 45^\circ$, in the start-up of steady shear flow. The shearing direction was changed two times. $v_x = \dot{\gamma}y$ for $\gamma = 0$ to $\gamma = 20$, $v_x = -\dot{\gamma}y$ for $\gamma = 20$ to $\gamma = -20$, and $v_x = \dot{\gamma}y$ for $\gamma = -20$ to $\gamma = 0$. (a) Fiber contribution to transient viscosity of the suspension $(\eta^+/\eta_s - 1)$; (b) normal stress coefficient difference $(\Psi_1^+ - \Psi_2^+)$; (c) first normal stress coefficient Ψ_1^+ ; and (d) second normal stress coefficient Ψ_2^+ .

present in the random system, which now is larger, and another very sharp one at $\gamma \approx 0.5$. The effect of the initial fiber orientation distribution on Ψ_1^+ is similar to that on $\Psi_1^+ - \Psi_2^+$. The peak

that is present in the random system increases its magnitude for suspensions with fibers uniformly aligned at $\phi_o = 90^\circ$ and $\theta_o = 90^\circ$. For suspensions with fibers aligned at $\phi_o = 90^\circ$ and $\theta_o = 45^\circ$, Ψ_2^+ is

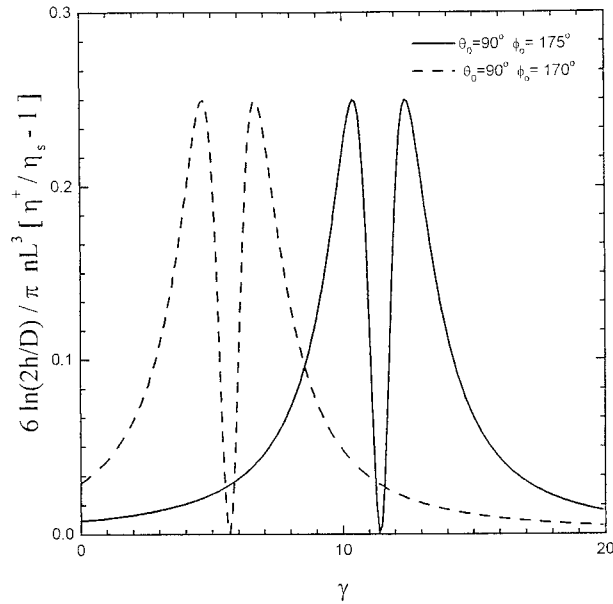


Figure 9. The dimensionless fiber contribution to the suspension viscosity as a function of shear strain for a suspension with uniform fiber orientation distribution. Two initial fiber orientations were used: $\phi_o = 175^\circ$, $\theta_o = 90^\circ$ (solid line) and $\phi_o = 170^\circ$, $\theta_o = 90^\circ$ (dashed line).

zero for all strains because for this specific orientation $\tau_{zz} = \tau_{yy}$ for all strains. All the rheological properties become independent of the initial fiber orientation distribution for $\gamma > 10$ and $\gamma < -10$. The sign change observed in the normal stress coefficients when the flow is reversed is not affected by the initial orientation distribution.

Figures 6, 7, and 8 have shown that there is an important difference in the rheological behavior between suspension with random orientations of fiber and suspension with uniform fiber orientation. This would indicate that by measuring the suspensions rheological properties using the flow history described above, we can predict whether the suspension has a random fiber distribution or not. If this test is negative, that is, if we find evidence that the suspension has a uniform fiber orientation the next step is to determine the orientation angles ϕ_o and θ_o . To study this possibility we calculated the rheological properties of a suspension with uniform fiber orientation in the start-up of steady shear flow for different initial fiber orientations.

Figures 9 and 10 show η^+ and $\Psi_1^+ - \Psi_2^+$ respectively, as functions of the shearing strain for two initial fiber orientations, $\phi_o = 175^\circ$, $\theta_o = 90^\circ$ and $\phi_o = 170^\circ$, $\theta_o = 90^\circ$. The strains at which the rheological properties have peaks are sensitive to

ϕ_o . The transient behavior for both values of ϕ_o is identical but the curves are shifted along the strain axis. A five degree change in ϕ_o around $\phi_o = 170^\circ$ produces a shift of approximately six strain units in all the rheological properties.

In Figure 11 we show $\Psi_1^+ - \Psi_2^+$ as a function of the shearing strain for two initial fiber orientations, $\phi_o = 175^\circ$, $\theta_o = 90^\circ$, and $\phi_o = 175^\circ$, $\theta_o = 85^\circ$. The magnitude of $\Psi_1^+ - \Psi_2^+$ is sensitive to θ_o , in as much as a five degree change in θ_o produces a variation of approximately one order of magnitude in the second and third peak of $\Psi_1^+ - \Psi_2^+$.

CONCLUSIONS

The introduction of fibers into a Newtonian fluid modifies its rheological properties because the fibers are rigid. In a homogeneous shear flow the fiber center of mass moves affinely with the fluid. The fiber cannot stretch; therefore, the velocity at any point along its axis, other than the center of mass, is different to the velocity of the undisturbed fluid. The velocity gradient in a fluid layer close to the fibers generates stresses that induce a force on the fibers, which is the origin of all the rheological properties of the suspension.

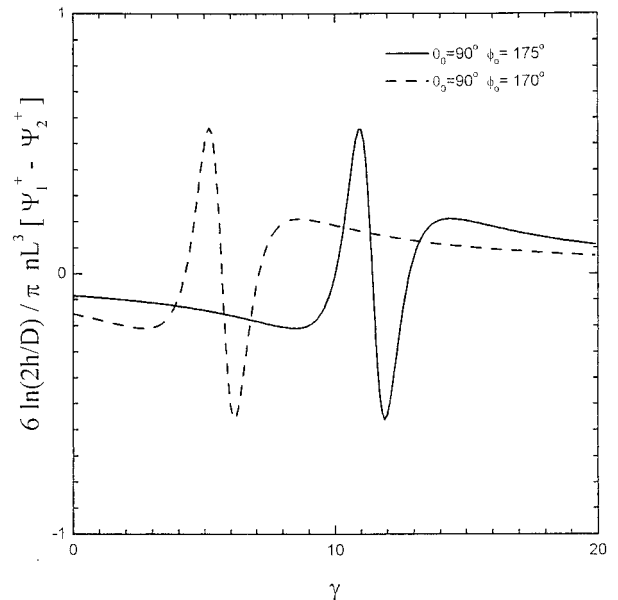


Figure 10. The dimensionless normal stress coefficient difference as a function of shear strain for a suspension with uniform fiber orientation distribution. Two initial fiber orientations were used: $\phi_o = 175^\circ$, $\theta_o = 90^\circ$ (solid line) and $\phi_o = 170^\circ$, $\theta_o = 90^\circ$ (dashed line).

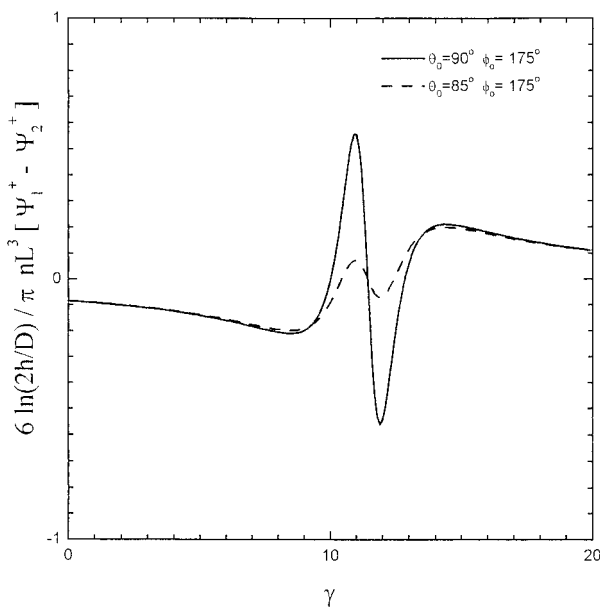


Figure 11. The dimensionless normal stress coefficient difference as a function of shear strain for a suspension with uniform fiber orientation distribution. Two initial fiber orientations were used: $\phi_0 = 175^\circ$, $\theta_0 = 90^\circ$ (solid line) and $\phi_0 = 175^\circ$, $\theta_0 = 85^\circ$ (dashed line).

The fiber motion was analyzed by two equations: The equation of motion proposed by Dinh and Armstrong predicts that after the start-up of steady shear flow, for $\gamma > 20$, the fibers are aligned in the shearing plane and stay in this plane forever, while the equation of motion derived by Jeffery, which is valid for very dilute suspensions in Newtonian fluids and can be used for any fiber aspect ratio, describes how the fibers go in and out of the shearing plane.

For large aspect ratio the fiber motion described by the Dinh and Armstrong equations is very close to that obtained using Jeffery's equation. We show clearly that for suspensions of long fibers, $L/D > 20$, the flipping time is so small compared with the time that the fiber remains in the shearing plane that for large strain, $\gamma > 20$, the overall picture is one of a suspension with all the fibers aligned in the shearing direction. On the other hand, for suspensions of short fibers, $L/D < 20$, both times are of the same order of magnitude and for large strain all fiber orientations are present.

This study has shown that, at least theoretically, the rheological properties of the suspension can be used to determine the fiber orientation in the sample. The first normal stress coefficient is the property to measure in order to determine

whether or not the suspension has a random fiber orientation. Eventually any of the three properties can be used to determine ϕ_0 and θ_0 but the first normal stress coefficient is the most sensitive to changes in these angles. The strain at one of the peaks can be used to calculate ϕ_0 ; and from the value of the magnitude of the property, θ_0 can be obtained. It was found that the normal stress coefficients can show negative or positive values depending on orientation of the fibers.

The authors gratefully acknowledge the financial support of the National Council of Argentina (CONICET).

REFERENCES AND NOTES

1. Jeffery, G. B. *Proc R Soc London* 1922, A102, 161.
2. Batchelor, G. K. *J Fluid Mech* 1970, 44, 419.
3. Batchelor, G. K. *J Fluid Mech* 1971, 46, 813.
4. Dinh, S. M.; Armstrong, R. C. *J Rheol* 1984, 28, 207.
5. Bibbó, M. A. Ph.D. Thesis, Massachusetts Institute of Technology, Cambridge, 1987.
6. Bibbó, M. A.; Dinh, S. M.; Armstrong, R. C. *J Rheol* 1985, 29, 905.
7. Barbosa, S. E. Ph.D. Thesis, Universidad Nacional del Sur, Bahia Blanca, Argentina, 1992.
8. Malamataris, N.; Papanastasiou, T. C. *J Rheol* 1991, 35, 449.
9. Barbosa, S. E.; Ercoli, D. R.; Bibbó, M. A.; Kenny, J. M. *Composite Structures* 1994, 27, 83.
10. Altan, M.; Subbiah, S.; Selcuk, A.; Pypes, R. B. *Polym Eng Sci* 1990, 30, 848.
11. Ausias, G.; Agassant, J.; Vincent, M.; Lafleur, P.; Lavoie, P.; Carreau, P. J. *J Rheol* 1992, 36, 525.
12. Folgar, F. P.; Tucker, C. L. *J Reinf Plast Compos* 1984, 3, 98.
13. Kamal, M. R.; Mutel, A. T. *Polym Compos* 1989, 10, 337.
14. Shaqfeh, E. S.; Frederickson, G. H. *Phys Fluids A* 1990, 2, 7.
15. Ranganathan, S.; Advani, S. G. *J Rheol* 1991, 35, 1499.
16. Bercraft, M. L.; Metzner, A. B. *J Rheol* 1992, 36, 143.
17. Doi, M. *J Polym Sci Polym Phys Ed* 1981, 19, 229.
18. Doraiswamy, D.; Metzner, A. B. *Rheol Acta* 1986, 36, 143.
19. Ghosh, T.; Grmela, M.; Carreau, P. J. *Polym Compos* 1995, 16, 144.
20. Okagawa, A.; Mason, S. G. *J Colloid Interface Sci* 1973, 45, 330.
21. Okagawa, A.; Cox, R. G.; Mason, S. G. *J Colloid Interface Sci* 1973, 45, 303.
22. Doi, M.; Edwards, S. F. *J Chem Soc Faraday Trans II* 1978, 74, 560.
23. Doi, M.; Edwards, S. F. *J Chem Soc Faraday Trans II* 1978, 74, 918.